



Available online at [www.sciencedirect.com](http://www.sciencedirect.com)



ScienceDirect

Trans. Nonferrous Met. Soc. China 28(2018) 1593–1601

Transactions of  
Nonferrous Metals  
Society of China

[www.tnmsc.cn](http://www.tnmsc.cn)



## Fretting wear behavior of Ti/TiN multilayer film on uranium surface under various displacement amplitudes

Yan-ping WU<sup>1</sup>, Zheng-yang LI<sup>2</sup>, Wen-jin YANG<sup>2</sup>, Sheng-fa ZHU<sup>1</sup>, Xian-dong MENG<sup>1</sup>, Zhen-bing CAI<sup>2</sup>

1. Institute of Materials, China Academy of Engineering Physics, Mianyang 621900, China;  
2. Tribology Research Institute, Key Laboratory of Advanced Materials Technology, Ministry of Education,  
Southwest Jiaotong University, Chengdu 610031, China

Received 24 April 2017; accepted 3 January 2018

**Abstract:** Ti/TiN multilayer film was deposited on uranium surface by arc ion plating technique to improve fretting wear behavior. The morphology, structure and element distribution of the film were measured by scanning electric microscopy (SEM), X-ray diffractometry (XRD) and Auger electron spectroscopy (AES). Fretting wear tests of uranium and Ti/TiN multilayer film were carried out using pin-on-disc configuration. The fretting tests of uranium and Ti/TiN multilayer film were carried out under normal load of 20 N and various displacement amplitudes ranging from 5 to 100  $\mu\text{m}$ . With the increase of the displacement amplitude, the fretting changed from partial slip regime (PSR) to slip regime (SR). The coefficient of friction (COF) increased with the increase of displacement amplitude. The results indicated that the displacement amplitude had a strong effect on fretting wear behavior of the film. The damage of the film was very slight when the displacement amplitude was below 20  $\mu\text{m}$ . The observations indicated that the delamination was the main wear mechanism of Ti/TiN multilayer film in PSR. The main wear mechanism of Ti/TiN multilayer film in SR was delamination and abrasive wear.

**Key words:** Ti/TiN multilayer film; fretting wear; wear mechanism; displacement amplitude

### 1 Introduction

Uranium has been extensively applied in nuclear power plant equipment and nuclear devices due to its special material and nuclear properties [1]. In order to satisfy the engineering design, uranium will inevitably contact or fasten with other materials, among which the contact interface is proved to bear different stress and have relative clearance. While in transport and service, uranium will be frequently affected by vibration, which leads to the relative motion with small displacement amplitude [2,3]. Fretting wear occurs when two contacting parts are subjected to small amplitude oscillatory sliding [4]. Fretting wear causes the initiation of fatigue crack, which limits the lifetime of the components [5,6].

Surface modification technique is an effective method to improve the wear-resistant properties of industry components [7,8]. Ti/TiN multilayer film has

attracted much attention to enhance mechanical properties and wear resistance, so it has been widely used in the field of cutting tools and some parts of engines [9–11]. Fretting is very sensitive to normal load [12], displacement amplitude [13], frequency [14], and environment [15,16].

SRINIVASANA et al [17] investigated the tribological behaviour of TiN, TiN/CrN, and Ti/TiN multilayer films on different substrates, and found that the Ti/TiN multilayer film shows a better wear resistance with all three substrates, as compared to TiN/CrN and TiN. ALI [18] used the numerical model of Ti/TiN multilayer film to find the optimal thickness of individual layers in a multilayer. The results show an increase in scratch adhesion of 18% and 27% for the optimal position and thickness of interlayers, respectively. The wear resistances of TiN, TiN gradient and Ti/TiN multilayer on uranium were investigated [19–21]. ZHANG et al [22] investigated the fretting wear and fretting fatigue behavior of Ti/TiN multilayer on Ti-811

**Foundation item:** Projects (U1530136, 51375407) supported by the National Natural Science Foundation of China; Project (2017TD0017) supported by the Young Scientific Innovation Team of Science and Technology of Sichuan Province, China

**Corresponding author:** Zhen-bing CAI; Tel: +86-28-87600601; E-mail: [czb-jiaoda@126.com](mailto:czb-jiaoda@126.com)  
DOI: 10.1016/S1003-6326(18)64801-0

alloy deposited by magnetron sputtering. Results show that Ti/TiN multilayer can significantly improve the resistance to fretting wear and fretting fatigue behavior of Ti-811 alloy at 350 °C due to its good toughness and high bonding strength. However, there are few studies on the fretting wear resistance of Ti/TiN multilayer films. So, it is meaningful to study the fretting behavior of Ti/TiN multilayer film on uranium.

In this study, Ti/TiN multilayer film was deposited on uranium surface by arc ion plating technology. The motivation of this report is to investigate the fretting behavior of Ti/TiN multilayer film and uranium under different displacement amplitudes. At the end of tests, the wear scars were examined by laser confocal scanning microscopy (LCSM), SEM and energy dispersive microscopy (EDS). The fretting behavior and mechanism of Ti/TiN multilayer film were discussed.

## 2 Experimental

### 2.1 Ti/TiN multilayer preparation

The substrate material used in the present study was uranium, which was usually used as nuclear weapons and nuclear power plants. It was ground, polished and ultrasonically cleaned in acetone and alcohol. The preparation of Ti/TiN multilayer film was carried out on arc ion plating equipment. The target was high purity Ti (99.99%). The samples were mounted on a continuously rotating planetary holder inside the vacuum chamber. Prior to deposition, the samples were further cleaned by argon ion bombardment. After the base pressure was pumped to be lower than  $5 \times 10^{-4}$  Pa, the working pressure was kept at 0.3 Pa. With the alternative atmosphere of pure argon and mixed argon and nitrogen controlled by mass flowmeters, the deposition procedures of Ti and TiN were repeated to prepare Ti/TiN multilayer film. For Ti layer, argon (99.999%) was introduced into the chamber with a flow of 40 mL/min. For TiN layer, argon (99.999%) and nitrogen (99.999%) were introduced into the chamber with flow rates of 10 and 40 mL/min. The target power was 2 kW. The deposited time of Ti and TiN was 5 and 10 min for each layer, respectively. The total deposited time was 1 h. The bias voltage was -180 V pulsed bias superposed by DC bias of -50 V.

### 2.2 Film characterization

The surface and cross-section morphologies were observed by SEM. The elastic modulus was evaluated by using nano-indentation of Hysitron Company under the force of 5 mN. Six points were chosen to obtain the average value. The structure of Ti/TiN multilayer film was investigated by XRD with Cu K $\alpha$  radiation ( $\lambda=0.15406$  nm). Scanning was carried out in the grazing angle mode with an incident beam angle of 2°. AES

depth profile was used to analyze the distribution of Ti and N elements. AES instrument model was PHI650 SAM, the excitation energy was 3 keV, the electron beam current was 100 nA, and the sputtering area was 1 mm<sup>2</sup>.

### 2.3 Fretting tests

The fretting tests were carried out on an MFT-6000 machine (Fig. 1). A pin-on-disc configuration was employed. The counter-body was a GCr15 ball with Ti/TiN multilayer film deposited as the samples. The diameter was 12 mm. During the test, the instantaneous displacement was monitored by laser copolymerization sensor with an accuracy of  $\pm 1$   $\mu$ m for every cycle. The normal force and tangential force were measured by three-dimensional pressure sensor. The experimental parameters were selected as displacement amplitudes of 5, 10, 20, 50 and 100  $\mu$ m, the frequency of 10 Hz, and the normal load of 20 N. The number of cycles was  $1 \times 10^4$ . The fretting tests were conducted in dry conditions at an ambient temperature of 25 °C and relative humidity of 50%. Prior to the fretting tests, the samples and counter-body were cleaned with acetone and alcohol. After each test, the morphologies of the wear scars were observed by LCSM and SEM. The profiles and wear volumes of the fretting scars were assessed using 3D optical microscope. The EDS was used to analyze the oxidation behavior of wear tracks.

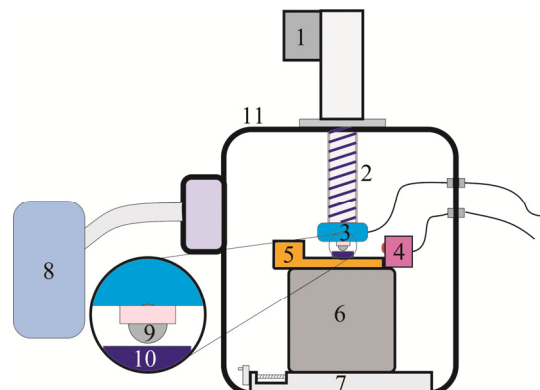


**Fig. 1** Fretting wear test rig: 1—Servo electric cylinder; 2—Lead screw; 3—Two-dimensional pressure sensor; 4—Laser copolymerization sensor; 5—Piezoelectric ceramics; 6—Base; 7—Screw module; 8—Vacuum pump group; 9—Ball sample; 10—Plate sample; 11—Vacuum chamber

## 3 Results and discussion

### 3.1 As-deposited film

The surface and cross-section morphologies of Ti/TiN multilayer film prepared by arc ion plating technology are shown in Fig. 2. From Fig. 2(a), the surface was globally uniform with some domes. The film was densely packed, no voids or micro-cracks in the

surface image (Fig. 2(a)). Cross-section images showed non-columnar structures (Fig. 2(b)). There were 4 bilayers with sharp interface, which were adhered well to the substrate. The average elastic modulus obtained by nano-indentation test under 5 mN was 471.55 GPa.

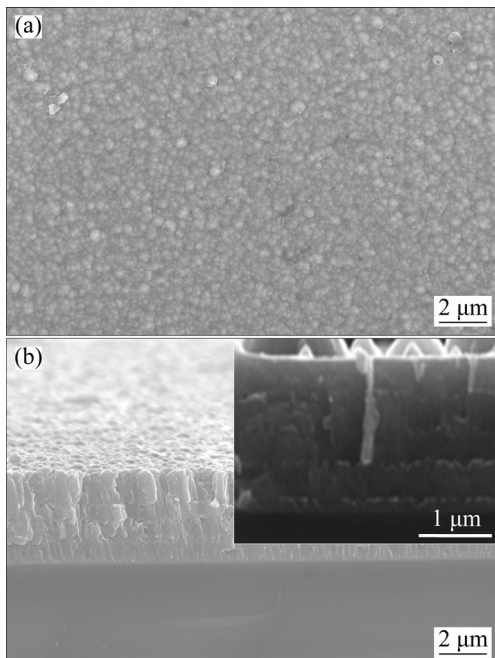


**Fig. 2** SEM morphologies of surface (a) and cross-section (b) of Ti/TiN multilayer film

The thickness of prepared film was about 2.27  $\mu\text{m}$ . To evaluate their phase structure, XRD analyses were performed with an incident angle of 2°. Figure 3 shows the XRD patterns of uranium and Ti/TiN multilayer film. There appeared primarily Ti phase and TiN phase. XRD patterns revealed a NaCl type face-centered cubic (FCC) structure with (111), (200) and (220) textures. Ti/TiN multilayer film was crystallized well. No other distinct diffraction peak was observed. The XRD pattern also revealed the existence of  $\alpha$ -U diffraction peak on the substrate.

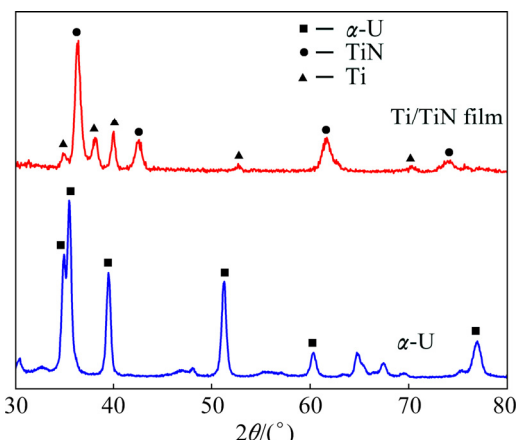


**Fig. 3** XRD patterns of uranium and Ti/TiN multilayer film

Ti and N element distribution in Ti/TiN multilayer film etched with 3 keV  $\text{Ar}^+$  for 22 min by AES is illustrated in Fig. 4. From the AES curves, it was found that, the molar fractions of Ti and N elements fluctuated periodically. When the content of Ti reached the maximum value, the content of N decreased to the minimum value. The N content was seen to increase gradually from the Ti layer to the TiN layer. On the initial surface, the content of N element was very high. With increase of the  $\text{Ar}^+$  etching time, the content of N element decreased quickly, which showed that a part of N element came from the surface contaminants. The thickness of 2.27  $\mu\text{m}$  was distributed in 4 bilayer periods.

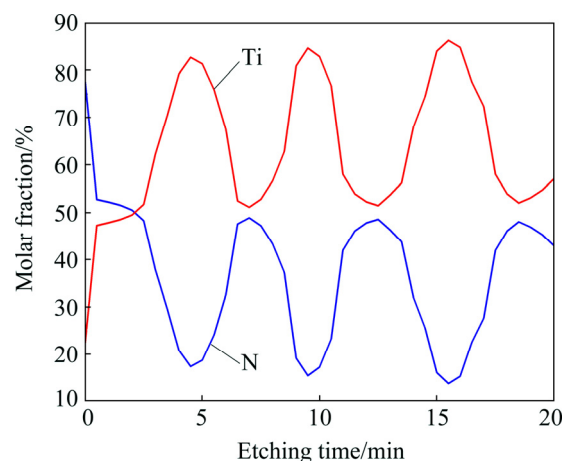


**Fig. 4** Ti and N elements distributions of Ti/TiN multilayer film measured by AES

### 3.2 Fretting properties

#### 3.2.1 Coefficient of friction

To evaluate the fretting wear of Ti/TiN multilayer film at different displacement amplitudes, the experimental parameters were selected as normal load of 20 N, the frequency of 10 Hz, displacement amplitudes of 5, 10, 20, 50 and 100  $\mu\text{m}$ , and the cycle number of  $1 \times 10^4$ . Figure 5 exhibits the evolution of the COF for uranium substrate and Ti/TiN multilayer film with the number of cycles at different displacement amplitudes. A great difference on COF was observed under different displacement amplitudes. The COF of uranium substrate or Ti/TiN multilayer film increased with the increase of test displacement. The COF of Ti/TiN multilayer film increased from 0.1 at the displacement amplitude of 5  $\mu\text{m}$  to 0.6 at the displacement amplitude of 50  $\mu\text{m}$ . At higher displacement amplitude, a large variation in COF was observed. When the displacement amplitude was less than 20  $\mu\text{m}$ , the COF obviously increased in the initial period of fretting wear and gradually tended to be a steady-state value, which was dependent on displacement amplitude. When the displacement amplitude was more than 50  $\mu\text{m}$ , the variation of COF was much higher. COF increased slowly with the number

of cycle at the beginning and reached the value of 0.6 after 5000 cycles.

### 3.2.2 Running condition of fretting loops

The fretting loops of uranium substrate and Ti/TiN multilayer film at a normal load of 20 N, displacement amplitudes of 5, 20 and 100  $\mu\text{m}$ , respectively, are shown in Fig. 6. Under an imposed normal load of 20 N, at low displacement amplitude, such as 5 and 20  $\mu\text{m}$  (see Figs. 6(a) and (b)), the shapes of tangential force–displacement ( $F$ – $D$ ) curves were elliptical loops and linear in all test cycles. The fretting loop remained almost unchanged as the number of fretting wear cycles

increased to  $1 \times 10^4$ , which was consistent with COF. Therefore, the fretting processes ran in PSR [23,24].

For the higher displacement amplitude ( $D=100 \mu\text{m}$ , see Fig. 6(c)), all  $F$ – $D$  curves were open as parallelogram and relative slip took place, which was the classic feature of SR [25,26]. The fretting loop increased to a higher friction value as the number of fretting wear cycles increased. The area of the fretting loop was the dissipated energy of friction. The dissipated energy of uranium substrate or Ti/TiN multilayer film increased with increasing the displacement amplitude. Ti/TiN multilayer film had a larger dissipated energy than

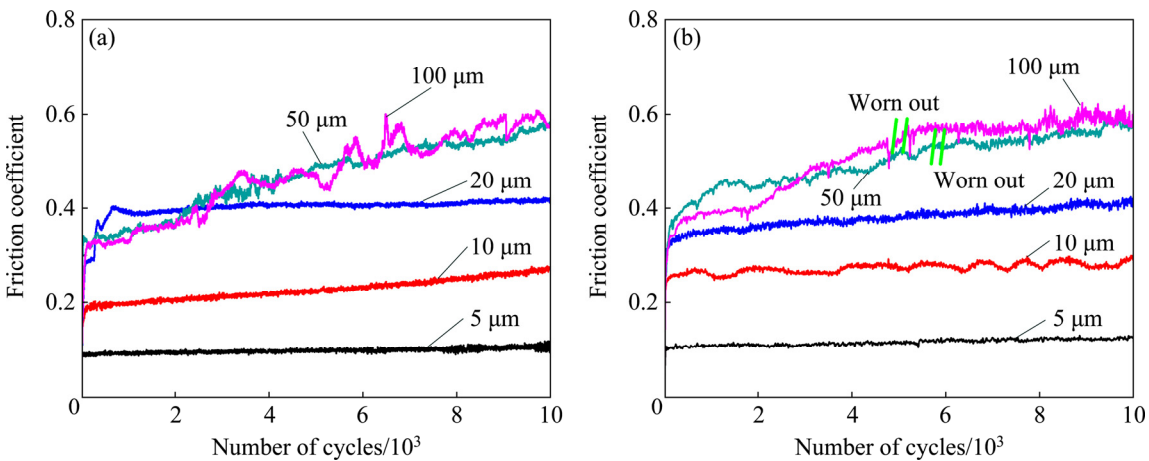


Fig. 5 Friction coefficients for uranium (a) and Ti/TiN multilayer film (b) at different displacement amplitudes

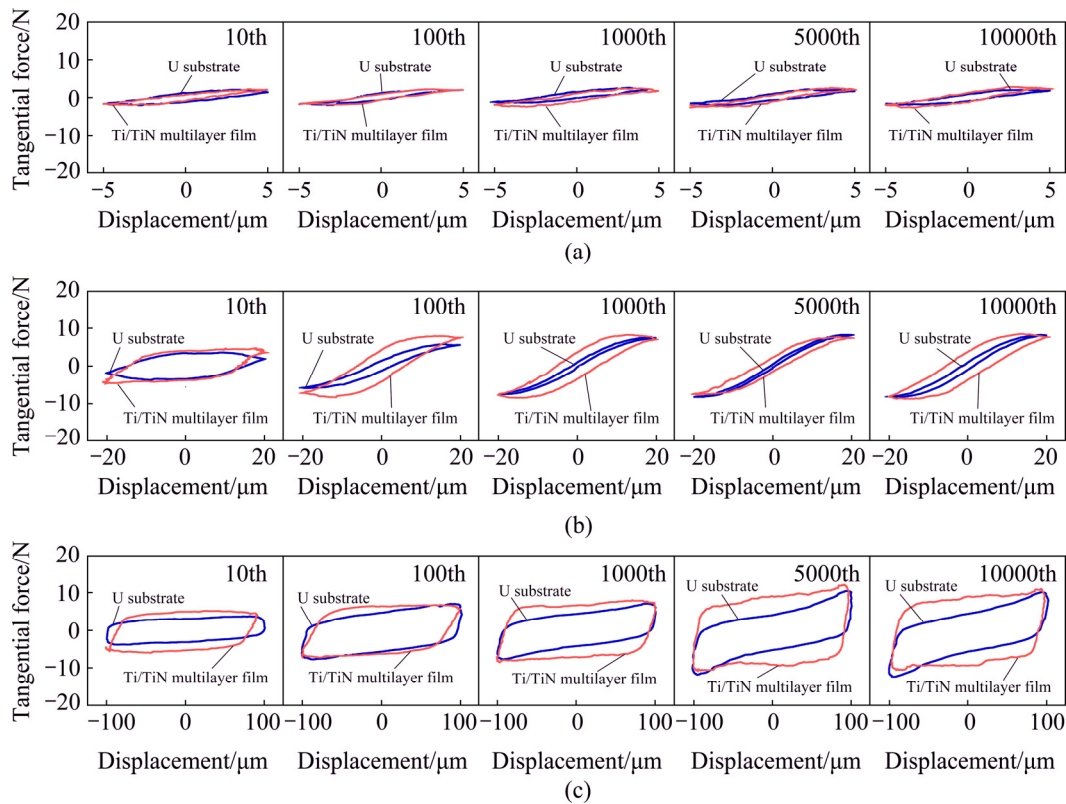


Fig. 6 Fretting loops for uranium and Ti/TiN multilayer film at normal load of 20 N and various displacement amplitudes: (a) 5  $\mu\text{m}$ ; (b) 20  $\mu\text{m}$ ; (c) 100  $\mu\text{m}$

uranium under different displacement amplitudes.

### 3.2.3 Damage observations and wear mechanism

Figure 7 shows optical morphologies of typical wear scars at a normal load of 20 N, displacement amplitude of 10, 20, 50 and 100  $\mu\text{m}$ , respectively. As can be seen from Fig. 7, when the displacement amplitude was smaller than 50  $\mu\text{m}$ , the shapes of wear scars were nearly round; when the displacement amplitude was 100  $\mu\text{m}$ , the worn scars were in ellipsoidal shape along the fretting direction. The size of wear scar increased with displacement amplitude increasing from 10 to 100  $\mu\text{m}$ . The wear scar for the displacement amplitude of 5  $\mu\text{m}$  was not found from the optical microscopy, which was observed from the SEM image (see Fig. 8(a)). A typical annular scar morphology of PSR was observed on the Ti/TiN multilayer film at the displacement amplitude of 10  $\mu\text{m}$ . With the increase of displacement amplitude, slide occurred over the entire surface. The wear damage increased with the increase of the displacement amplitude. At higher displacement amplitudes ( $D=50$  and 100  $\mu\text{m}$ , see Figs. 7(c) and (d), respectively), the stick zone disappeared, and the substrate materials of uranium emerged. At the edge of wear scar, the layered structure damage was found in the Ti/TiN multilayer film, as seen in the annular morphology.

To analyze the wear damage, the SEM images and EDS analysis of Ti/TiN multilayer film are presented in

Fig. 8. It was observed that Ti/TiN multilayer film only presented slight scratch when displacement amplitude was 5  $\mu\text{m}$  (Figs. 8(a, b)). Some lamellate plates also presented in fretting scar (at the contact edge of the wear region), which came from the counter ball. No damage was observed at the contact center when the displacement amplitude was small.

When the displacement amplitude was 20  $\mu\text{m}$ , the fretting wear ran in PSR. A few detached particles covering in the contact zone formed third-body contact. The lamellate plates also presented in fretting scar. From the EDS spectra, at the center of wear scar, the dominant elements were Ti and N, with low content of O. At the edge of wear scar, O content increased with the decrease of the Ti and N contents. Ti and N elements presented as “W” shape, indicated that the edge of wear scar was partial slip zone and had a more tribochemical reaction with O. Ti/TiN multilayer film had much severer damage at the edge than at the center. The delamination was main wear mechanism.

A lot of particles were found on the surface when displacement amplitude was 100  $\mu\text{m}$  (Figs. 8(e, f)). A thick debris layer covered on the contact zones. At Spots 1 and 2, as indicated in Fig. 8(f), EDS analysis was carried out. The molar fractions were summarized in Table 1. In Spot 1, the main elements were Ti and N with little O, coming from the substrate. In Spot 2, the dominant elements were U and O at the edge of wear

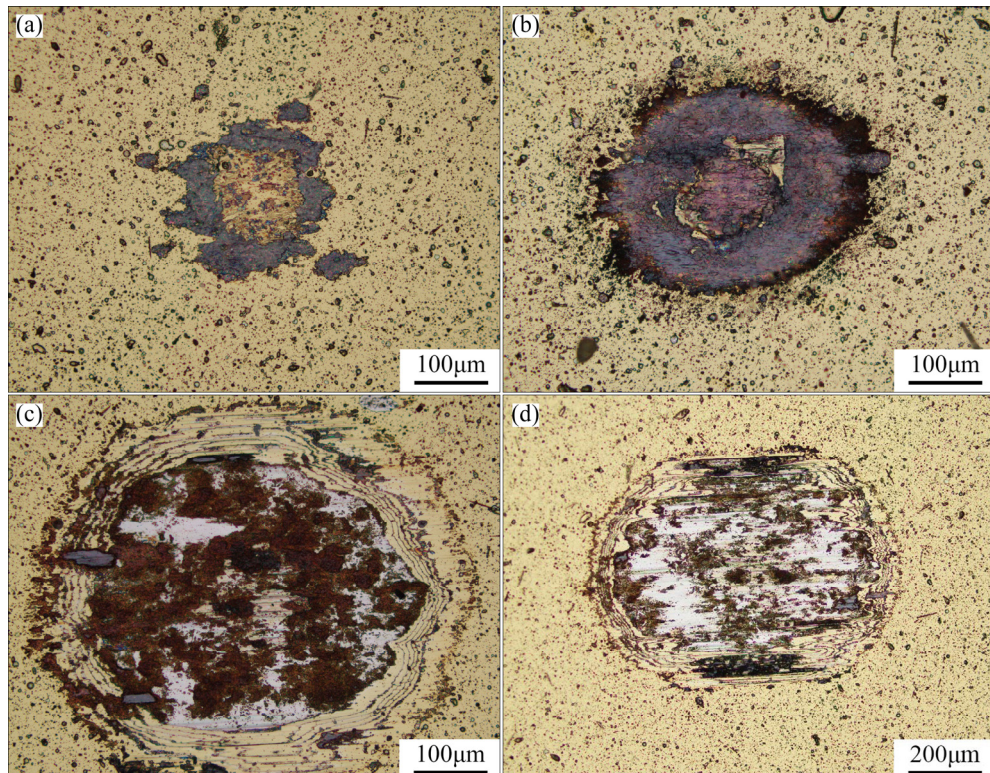


**Fig. 7** Optical morphologies of fretting damaged surfaces of Ti/TiN multilayer film at different displacement amplitudes: (a)  $D=10 \mu\text{m}$ ; (b)  $D=20 \mu\text{m}$ ; (c)  $D=50 \mu\text{m}$ ; (d)  $D=100 \mu\text{m}$

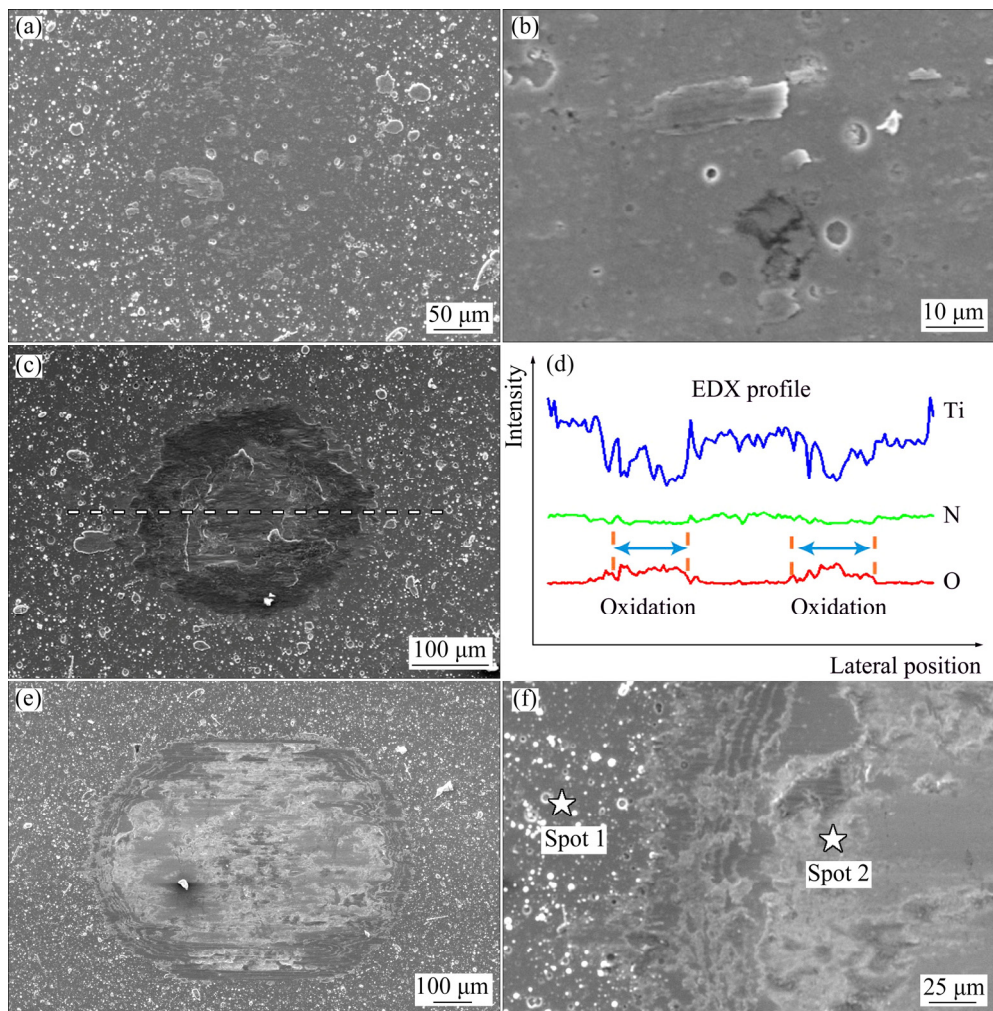


**Fig. 8** SEM morphologies of fretting damaged surface of Ti/TiN multilayer film: (a, b)  $D=5 \mu\text{m}$ ; (c, d)  $D=20 \mu\text{m}$ ; (e, f)  $D=100 \mu\text{m}$

**Table 1** EDS response at Spot 1 and 2 as indicated in Fig. 8(f)

Element	Molar fraction at Spot 1/%	Molar fraction at Spot 2/%
U	0.61	91.28
Ti	47.16	0.48
N	42.18	0.00
O	10.06	8.24

scar. The Ti/TiN multilayer film flaked off severely and caused uranium substrate to be exposed in air, which can be seen from the EDS spectra. Ti/TiN multilayer film was completely damaged due to gross sliding; the protection effect of the film was lost. Therefore, the COF value the Ti/TiN multilayer film was consistent with that of uranium substrate after 5000 cycles. The delamination and abrasive wear were main wear mechanism in SR.

Figure 9 presents scar profile of uranium and Ti/TiN multilayer film at normal load of 20 N, displacement amplitudes of 5, 10, 20, 50 and 100  $\mu\text{m}$ . The scar profiles were measured by 3D optical microscope. Profiles at

lower displacement amplitude presented very slight material transfer. At the displacement amplitudes of 5 and 10  $\mu\text{m}$ , the depth of wear scar in the center was less than the film thickness. The film removed incompletely from the contact zone although some scratch formed. The protection effect of the film still existed after  $1 \times 10^4$  cycles. The wear depth was larger than the film thickness when displacement amplitude was above 20  $\mu\text{m}$ .

Figure 10 shows the 3D profiles of Ti/TiN multilayer film under different displacement amplitudes. The wear area increased with the increase of displacement amplitude. At the displacement amplitude of 20  $\mu\text{m}$ , the wear debris was not discharged completely during the test, and the wear scar was bulgy partly. When the displacement amplitude increased to 50 and 100  $\mu\text{m}$ , respectively, the wear morphology was elliptic type. Because the wear debris could discharge easily from the wear scar, and the wear morphology was regular.

Figure 11 shows the wear volume and wear rate of uranium and Ti/TiN multilayer film at different displacement amplitudes. It could be found that the wear

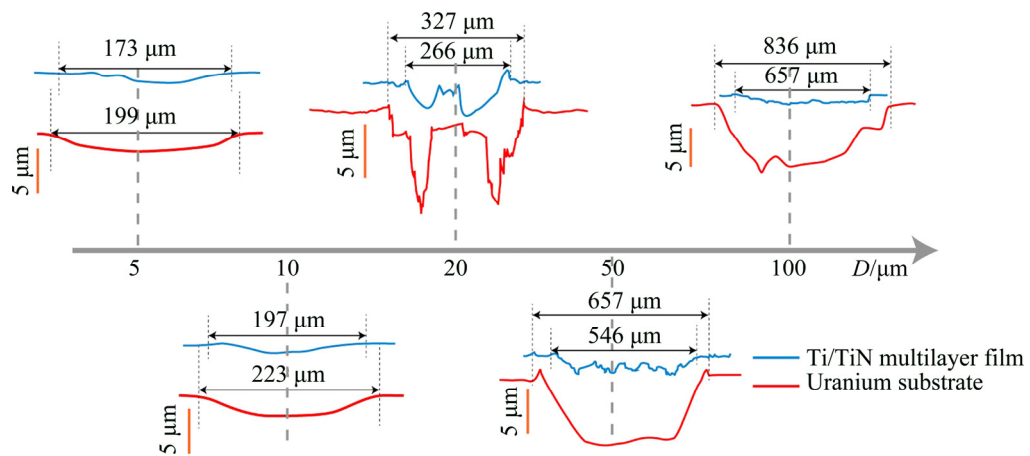


Fig. 9 Scar profiles of uranium and Ti/TiN multilayer film at different displacement amplitudes

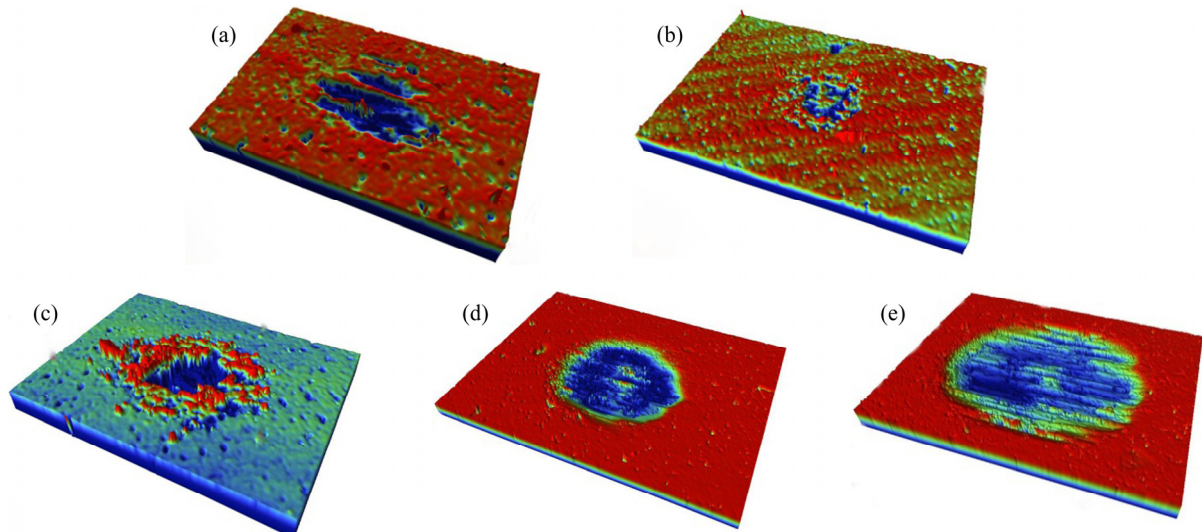


Fig. 10 3D profiles of Ti/TiN multilayer film at different displacement amplitudes: (a) 5  $\mu\text{m}$ ; (b) 10  $\mu\text{m}$ ; (c) 20  $\mu\text{m}$ ; (d) 50  $\mu\text{m}$ ; (e) 100  $\mu\text{m}$

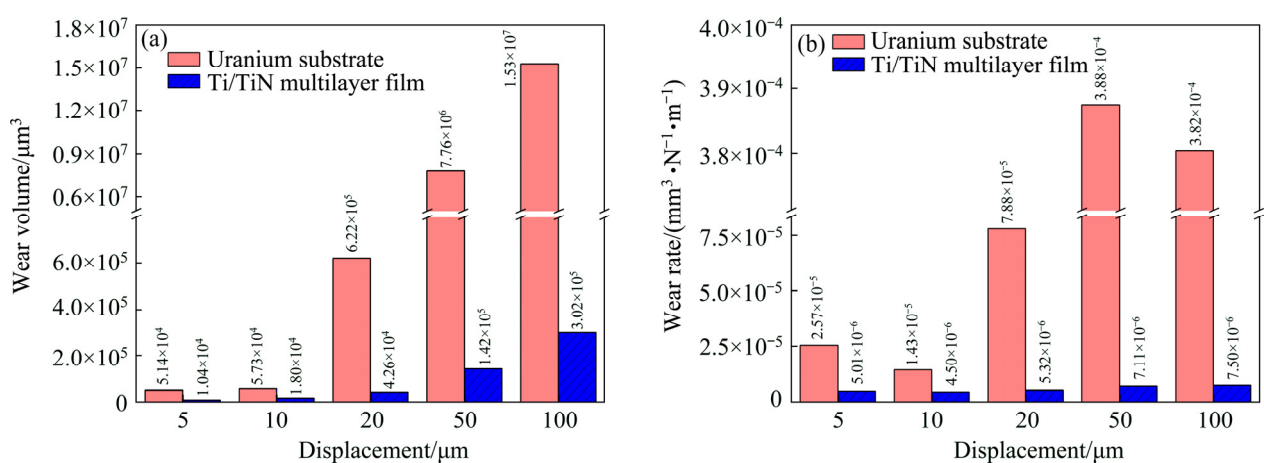


Fig. 11 Wear volume (a) and wear rate (b) of uranium and Ti/TiN multilayer film at different displacement amplitudes

volume gradually increased with the increase of displacement amplitude. The wear volume increased slowly when the displacement amplitude was lower than 10  $\mu\text{m}$ . A distinct increase of wear volume was observed when the displacement amplitude was above 20  $\mu\text{m}$ .

When the displacement amplitudes was 50  $\mu\text{m}$ , the wear rate was maximum. From the wear volume and wear rate, it was found that the Ti/TiN multilayer film could improve the tribological behaviors of uranium greatly.

## 4 Conclusions

1) The thickness of Ti/TiN multilayer film was about 2.27  $\mu\text{m}$ . The film was densely packed, and there were no voids and micro-cracks. The average elastic modulus obtained by nano-indentation test under 5 mN force was 471.55 GPa.

2) The fretting process ran in PSR and SR under different displacement amplitudes. With the increase of displacement amplitude, the depth and width of wear scars became larger due to transformation of the fretting mode from PSR to SR.

3) The delamination was main wear mechanism in the PSR. Abrasive and delamination were the main wear mechanism in the SR for the Ti/TiN multilayer film.

## Acknowledgments

The authors would like to thank Professor Min-hao ZHU for the useful advice, Xian'e TANG for optical microscopy observation, Ding-mu LANG for SEM investigation and Qin-guo WANG for XRD investigation.

## References

- [1] ZHU Sheng-fa, CHEN Lin, WU Yan-ping, HU Yin. Microstructure and corrosion resistance of Cr/Cr<sub>2</sub>N multilayer film deposited on the surface of depleted uranium [J]. Corrosion Science, 2014, 82(2): 420–425.
- [2] BAI Bin, XIAO Yun-feng, LANG Ding-mu, LIU Qing-he. Friction characteristics of plasma-sprayed Sn and ZrO<sub>2</sub> coatings against U–Nb alloy [J]. Rare Metal Materials and Engineering, 2005, 34(7): 1114–1118. (in Chinese)
- [3] WU Yan-ping, LI Zheng-yang, ZHU Sheng-fa, LU Lei, CAI Zhen-bing. Effect of frequency on fretting wear behavior of Ti/TiN multilayer film on depleted uranium [J]. PloS One, 2017, 12(4): e0175084.
- [4] ZHU Min-hao, ZHOU Zhong-rong. On the mechanisms of various fretting wear modes [J]. Tribology International, 2011, 44(11): 1378–1388.
- [5] ZHOU Zhong-rong, VINCENT L. Cracking induced by fretting of aluminium alloys [J]. Journal of Tribology, 1997, 119(1): 36–42.
- [6] PROUDHON H, FOUVRY S, YANTIO G R. Determination and prediction of the fretting crack initiation: Introduction of the (P, Q, N) representation and definition of a variable process volume [J]. International Journal of Fatigue, 2006, 28(7): 707–713.
- [7] LI Zheng-yang, CAI Zhen-bing, WU Yan-ping, ZHU Min-hao. Effect of nitrogen ion implantation dose on torsional fretting wear behavior of titanium and its alloy [J]. Transactions of Nonferrous Metals Society of China, 2017, 27(2): 324–335.
- [8] DU Dong-xing, LIU Dao-xin, ZHANG Xiao-hua, TANG Jin-gang, XIANG Ding-gen. Characterization and mechanical properties investigation of TiN–Ag films onto Ti–6Al–4V [J]. Applied Surface Science, 2016, 365: 47–56.
- [9] EZAZI M A, QUAZI M M, ZALNEZHAD E, SARHAN A A. Enhancing the tribomechanical properties of aerospace AL7075-T6 by magnetron-sputtered Ti/TiN, Cr/CrN and TiCr/TiCrN thin film ceramic coatings [J]. Ceramics International, 2014, 40(10): 15603–15615.
- [10] LIN Song-sheng, ZHOU Ke-song, DAI Ming-jiang, HU Fang, SHI Qian, HOU Hui-jun. Effects of surface roughness of substrate on properties of Ti/TiN/Zr/ZrN multilayer coatings [J]. Transactions of Nonferrous Metals Society of China, 2015, 25(2): 451–456.
- [11] MATOR L, LACKNER J M, MAJOR B. Bio-tribological TiN/Ti/a-C:H multilayer coatings development with a built-in mechanism of controlled wear [J]. RSC Advances, 2014, 4(40): 21108–21114.
- [12] WANG Shi-bo, CAO Bo. Torsion tribological behavior of polytetrafluoroethylene composites under dynamic normal load: Effect of dynamic normal load amplitude [J]. Tribology Transactions, 2016, 59(3): 462–468.
- [13] ZHANG Xiao-yu, REN Ping-di, ZHONG Fa-chun, ZHU Min-hao, ZHOU Zhong-rong. Fretting wear and friction oxidation behavior of 0Cr20Ni32AlTi alloy at high temperature [J]. Transactions of Nonferrous Metals Society of China, 2012, 22(4): 825–830.
- [14] WARMUTH A R, SHIPWAY P H, SUN W. Fretting wear mapping: The influence of contact geometry and frequency on debris formation and ejection for a steel-on-steel pair [J]. Proceedings of the Royal Society A: Mathematical Physical & Engineering Sciences, 2015, 471(2178): 20140291.
- [15] ESTEVES M, RAMALHO A, RAMOS F. Fretting behavior of the AISI 304 stainless steel under different atmosphere environments [J]. Tribology International, 2015, 88: 56–65.
- [16] CHEN H, WU P Q, QUAEYHAEGENS C, XU K W, STALS L M, HE J W, CELIS J P. Comparison of fretting wear of Cr-rich CrN and TiN coatings in air of different relative humidities [J]. Wear, 2002, 253(5–6): 527–532.
- [17] SRINIVASANA D, KULKARNIB T G, ANAND K. Thermal stability and high-temperature wear of Ti–TiN and TiN–CrN nanomultilayer coatings under self-mated conditions [J]. Tribology International, 2007, 40: 266–277.
- [18] ALI R, SEBASTIANI M, BEMPORAD E. Influence of Ti–TiN multilayer PVD-coatings design on residual stresses and adhesion [J]. Materials & Design, 2015, 75: 47–56.
- [19] LIU Tian-wei, DONG Chuang, WU Sheng, TANG Kai. TiN, TiN gradient and Ti/TiN multi-layer protective coatings on uranium [J]. Surface & Coatings Technology, 2007, 201(15): 6737–6741.
- [20] LIU Tian-wei, WANG Xiao-ying, JIANG Fan, TANG Kai. Structure and corrosion resistance of multi-layer Ti/TiN films prepared on uranium by arc ion plating under different bias voltages [J]. Atomic Energy Science & Technology, 2011, 45(8): 1020–1024.
- [21] CHENG Y H, BROWNE T, HECKERMAN B, BOWMAN C, GOROKHOVSKY V, MELETIS E I. Mechanical and tribological properties of TiN/Ti multilayer coating [J]. Surface & Coatings Technology, 2010, 205(1): 146–151.
- [22] ZHANG Xiao-hua, PAN Feng, XIANG Ding-gen. Characterization of fretting fatigue behavior of TiN/Ti Coating on Ti-811 alloy at increased temperature [C]// Proceedings of the First Symposium on Aviation Maintenance and Management–Volume II. Heidelberg: Springer, 2014: 699–705.
- [23] SHEN F, HU W, VOYIADIS G Z, MENG Q. Effects of fatigue damage and wear on fretting fatigue under partial slip condition [J]. Wear, 2015, 338: 394–405.
- [24] PAGGI M, POHRT R, POPOV V L. Partial-slip frictional response of rough surfaces [J]. Scientific Reports, 2014, 4(4): 5178–5183.
- [25] YUE T, WAHAB M A. Finite element analysis of stress singularity in partial slip and gross sliding regimes in fretting wear [J]. Wear, 2014, 321: 53–63.
- [26] ZHANG Xiao-yu, REN Ping-di, PENG Jin-fang, ZHU Min-hao. Fretting wear behavior of Inconel 690 in hydrazine environments [J]. Transactions of Nonferrous Metals Society of China, 2014, 24(2): 360–367.

# 铀表面 Ti/TiN 多层涂层在不同位移幅值下的微动磨损行为

吴艳萍<sup>1</sup>, 李正阳<sup>2</sup>, 杨文锦<sup>2</sup>, 朱生发<sup>1</sup>, 孟宪东<sup>1</sup>, 蔡振兵<sup>2</sup>

1. 中国工程物理研究院 材料研究所, 绵阳 621900;  
2. 西南交通大学 材料先进技术教育部重点实验室 摩擦学研究所, 成都 610031

**摘要:** 利用多弧离子镀技术在铀表面制备 Ti/TiN 多层涂层以提高其微动磨损性能。采用 SEM、XRD 和 AES 研究多层涂层的形貌、结构和元素分布。通过销/盘接触方式研究铀及 Ti/TiN 多层涂层的微动磨损行为。铀及 Ti/TiN 多层涂层的微动磨损测试条件为载荷 20 N、位移幅值 5~100  $\mu\text{m}$ 。随着位移幅值的增加, 微动运行从部分滑移区变为完全滑移区。摩擦因数随着位移幅值的增加而增加。结果表明, 位移幅值显著影响涂层的微动磨损性能。当位移幅值小于 20  $\mu\text{m}$  时, 涂层出现轻微损伤。研究表明, Ti/TiN 多层涂层在部分滑移区的主要磨损机理为剥层, 而在完全滑移区的磨损机理为剥层和磨粒磨损。

**关键词:** Ti/TiN 多层涂层; 微动磨损; 磨损机理; 位移幅值

(Edited by Wei-ping CHEN)